



The Norwegian University of Science and Technology  
Department of Computer Science  
Gjovik, Norway

---

Final Project for IDIG4002 – Computer Graphics Fundamentals and Applications - 7.5 credits

## WIDE-ANGLE IMAGE SIMULATION

Dong Han  
Email: [dongha@stud.ntnu.no](mailto:dongha@stud.ntnu.no)

Milan Kresović  
Email: [milank@stud.ntnu.no](mailto:milank@stud.ntnu.no)

Ronny Xavier Velastegui Sandoval  
Email: [ronnyxv@stud.ntnu.no](mailto:ronnyxv@stud.ntnu.no)

## 1. Introduction

Computer Graphics is a sub-field of Computer Science in charge of the creation and manipulation of 2D and 3D digital contents through mathematical models and computational algorithms. Generally, most researches in computer graphics focus on aspects such as geometry, lighting, textures, or shadows [1]. However, the camera models also play a very important role in providing more realism during the rendering process of the models. For this reason, the camera simulation is essential for application of computer graphics both in industrial and research fields. In specific, through lens camera simulations, we could be able to estimate the result of using different camera lenses before the production of their physical prototypes [2]. Additionally, using the results of these simulations, we could improve the realism in video games, movies, virtual reality, etc.

Focal distance is one of core parameters for any lens system. It is defined by the distance from focal point to the vertex of the lens. The shorter focal length means a wider field of view. This allows more objects in the scene to be shown in the image, but the size of each object decreases with respect to the final image. As showing in Figure 1, the field of view (FOV) is inversely proportional to the focal length. Therefore, there is also a "magnification" in the image when the FOV is narrow.

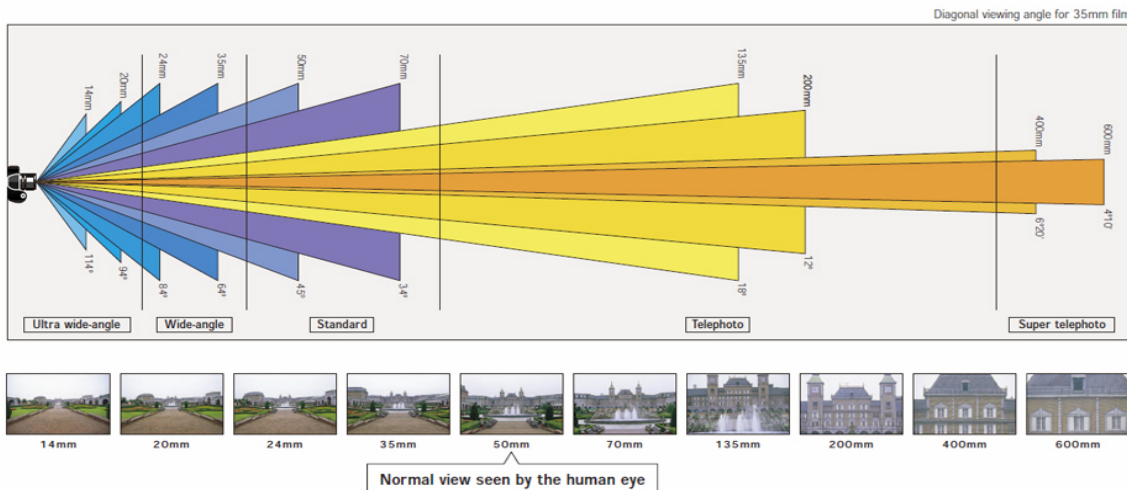


Figure 1: Relationship between focal length and field of view [3]

A wide-angle lens is any lens with a focal length shorter than the length of the sensor or film. For full frame sensors, a wide angle lens would be any lens with a focal length equal to or less than 35mm. Specifically, a lens system with a 50mm focal length is the one that most closely resembles the image captured by standard human eyes. Thus, it is for this reason that the camera focal length setting is crucial in movies and video games as it contributes to the realism of the perceived images.

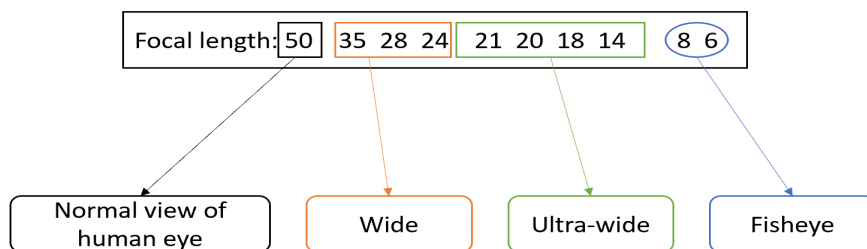


Figure 2: Focal lengths of most common cameras (mm)

For full-frame sensors 35mm camera, normal wide-angle lenses are defined by focal length from 24mm to 35mm. The ultra wide-angle lenses have a focal length shorter than the short side of the film or sensor. In this case, the focal length of ultra wide-angle lens is less than 24mm. The 21mm, 20mm, 18mm, 14mm are classical focal lengths for the ultra-wide lenses. In such shorter focal lengths range, some barrel distortion are introduced into the image. The barrel distortion is one type of optical aberration. Therefore, when the image is generated on the film, the image sensor cannot fit whole image, then the image will be squeezed [4]. Normally, the focal lengths of fish eye lenses are from 6mm to 8mm (in round image). In general, the image taken by a fisheye lens is quite deformed and has a strong sense of perspective convergence. The focal lengths from 8mm to 16mm can be used for designing ultra wide-angle lens camera as well as fisheye camera. This is indicated in Figure 2.

PBRT is a physically based rendering system in accordance with the ray-tracing algorithm. It attempts to make pictures of scene by developing models of light transport that are derived from physics. The basic computational framework combines vector math, coordinate transformations, basic operations of intersecting rays with geometric shapes, ray acceleration, the color radiometry, followed by camera models and sampling. Hence, according to all these concepts mentioned above, PBRT manages to render quite realistic scenes. In addition, when the reflection models, materials, lighting sources, texturing are involved in rendering procedure, it is called "physically based" rendering which is the basis and advantage of PBRT over other APIs [5].

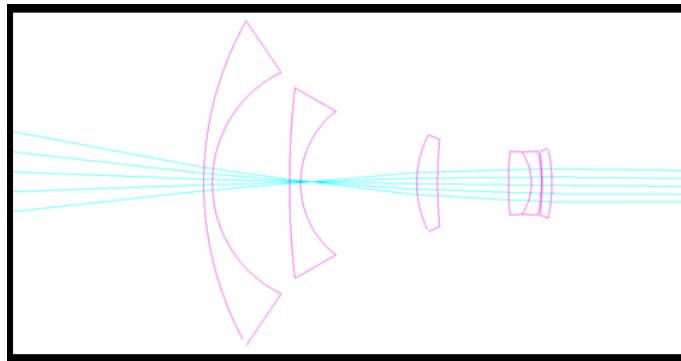


Figure 3: Muller 16mm/f4 155.9FOV Fisheye [6]

In regards to camera models, PBRT handles 4 main models: perspective, orthographic, environment and realistic. The realistic camera is a fairly realistic model which simulates light ray traveling through each single surface of lens to generate an image, which is similar with image taken by real cameras. The cross section of the Muller Fisheye lens system is shown in Figure 3. Assuming a conventional camera, the leftmost lens is the one closest to the object to be photographed, while the opposite lens corresponds to the side closest to the film. Generally, there is a aperture stop in lens system that controls exposure times and depth of field with adjustable size.

Muller's lens specifications, according to the PBRT Scene Library, are shown in Table 1. Each row in this table is called a lens interface, and it defines a surface of a single lens element. The rows are ordered according to Figure 3, going from left to right. The unit of those parameters are represented in millimeters. The curvature radius is the distance from the vertex to the center of curvature. If the surface is planar, then this value does not exist. Moreover, the values of curvature radius can be positive or negative. The positive value means that the surface is a convex if from the front of lens. The negative value indicates that the radius of the curvature is a concave. The second parameter is thickness, it is the distance from the surface to the adjacent surface and can be measured along the central axis. The next one is the index of refraction, and it depends which material is associated. Normally, this index is more than one for any type of lens. When there is a gap between two surfaces, if no specification is given, the medium is assumed to be air. The last one is the diameter of aperture, and it describes the vertical size of the lens above and below the optical axis.

Index	Curvature Radius	Thickness	Index of Refraction	Aperture Diameter
1	30.2249	0.8335	1.62	30.34
2	11.3931	7.4136	1	20.68
3	75.2019	1.0654	1.639	17.8
4	8.3349	11.1549	1	13.42
5	9.5882	2.0054	1.654	9.02
6	43.8677	5.3895	1	8.14
7	0	1.4163	0	6.08
8	29.4541	2.1934	1.517	5.96
9	-5.2265	0.9714	1.805	5.84
10	-14.2884	0.0627	1	5.96
11	-22.3726	0.94	1.673	5.96
12	-15.0404	0	1	6.52

Table 1: Tabular description of the PBRT Muller lens system, with 10mm focal distance.

In this work, we will implement a simulation of different wide-angle cameras using PBRT-V3 API. For this, we will start using as a base one of the realistic lenses available in the Scenes Library of PBRT-V3. Thus, through the systematic addition and removal of lens interfaces, we will create different wide-angle cameras with different FOV and Focal Length properties. So, we will explore different cameras with focal lengths from 50mm to 10mm, which produce fields of view from approximately 45 Degrees to 155 Degrees. In this way, we will be able to observe the transition from a camera with a standard field of view (50mm focal length) similar to the human eye, to a camera with an ultra-wide field of view (10mm focal length) similar to a fisheye. Thus, once those different wide-angle cameras have been generated, we will test them in different scenes. In this way, we will simulate the performance of our cameras in different environments, with different lighting conditions and viewing angles.

## 2. Methodology

For the methodology of our experiment, we will use as a base the lens system shown in Table 1. So, through an exhaustive combination of the different interfaces of this lens system, we noticed that, by sequentially removing or adding the lens interfaces, the produced FOV progressively decreases or increases. Based on this fact, we will start creating a very simple lens system taking just 3 lens interfaces of the base system. This new lens system will be our "Level 1" camera, and it is made up of the three interfaces with indices 6, 7, and 8 from Table 1 (Notice that the interface in position 7 corresponds to the aperture stop, and we will use it as the center of our system). Then, to generate the "Level 2" camera, we will add two interfaces (one on the left and one on the right) to the previous camera. And so on, until completing the system that is shown in Table 1. So, in the final, we will generate 6 files of cameras each with a different FOV value. In Figure 4, we can see the result of using each of the realistic cameras generated with this method.

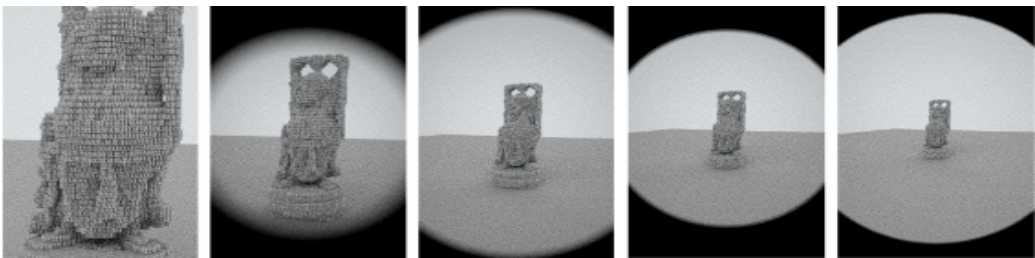


Figure 4: Different wide-angle cameras generated. The level 1 is located on the left side, while the level 5 is located on the right side

Thus, following this methodology, we noticed that as we went from Level 1 to Level 5, the FOV of the rendered image increased, obtaining a more wide-angle camera at each level. So, the Level 1 camera corresponds approximately to the standard human field of view, while the Level 5 camera corresponds to an ultra-wide FOV similar to a fisheye. Note that this trend is met with all the 5 levels, but with the only exception of one extra level which is not shown in Figure 4. Thus, this level was between the current level 3 and 4, but this was removed from our methodology because it did not correspond to a wide-angle type camera. Therefore, we will omit the analysis of this discarded level as it does not belong to the main focus of our work about wide-angle cameras. Consider that we can allow this omission in our methodology since our objective is not to find a strict relationship between the number of lens interfaces and the FOV obtained, but simply to simulate different types of wide-angle cameras with different FOVs and test them in different scenes conditions.

So, to test our 5 different cameras, we will render two main scenes from the PBRT-V3 Scene Library. The first scene corresponds to an example of an Indoor environment, while the second scene corresponds to an example of an Outdoor environment. This is important, since it will allow us to appreciate the sensation of variation in the depth of field, and it will also allow us to appreciate how the number of elements visible on the screen increases as the FOV increases. Also, in both scenes we will modify the lighting conditions, thus simulating both intense light conditions and dim light conditions. Finally, we will also modify the position and direction of the camera to test different viewing angles. In this way, we will observe the performance of our wide-angle cameras under these different scene conditions.

### 3. Results

As it was explained before, in order to test the created wide-angle lens systems, two different scenes were used. One represents the indoor environment, while the other represents the outdoor environment. The scenes were found in the PBRT v3 scenes repository [7]. The specific scenes that were used for indoor and outdoor environment are "contemporary-bathroom" [8] and "ecosys" [9], respectively. The rendering of these scenes can be appreciated in Figure 5.

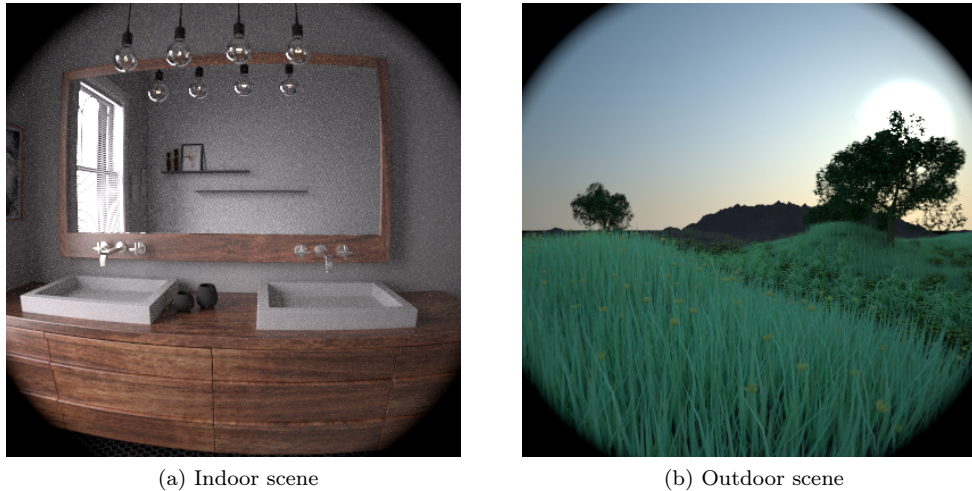


Figure 5: Two different scenes used for testing the wide-angle lens systems

In order to test how light affects the created lens systems, different types of lighting conditions were utilized. The main objective was to show the behavior of the lens system in the high and low brightness environment. The morning lighting conditions were used for the high brightness environment, whereas the dusk lighting was used for the low brightness environment. The example rendering can be observed in Figure 6.

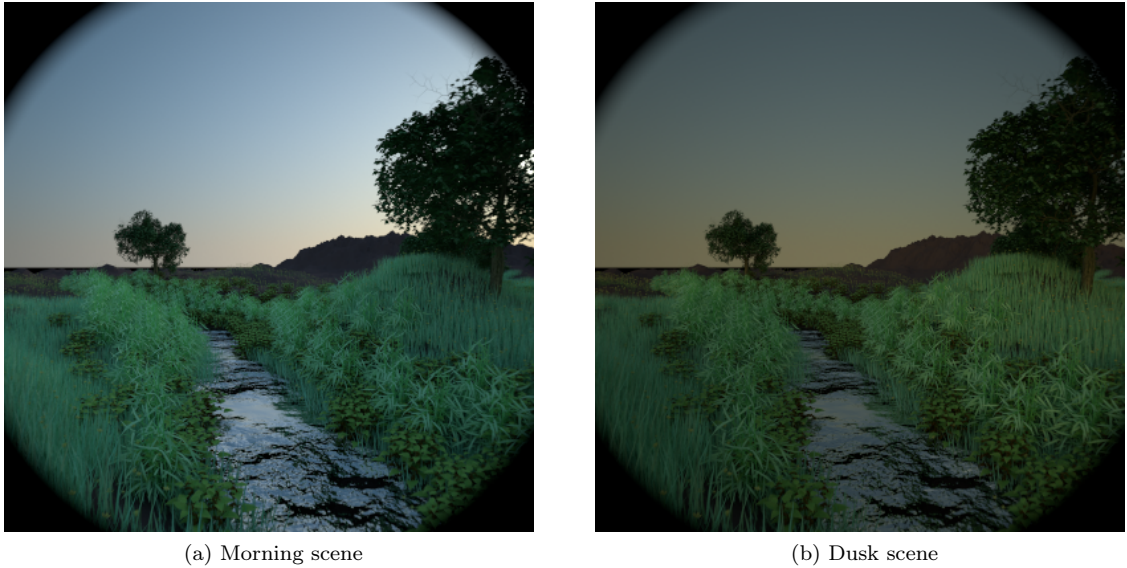


Figure 6: Testing the behavior of the wide-angle lens systems under different lighting

In Figure 6, it can be observed that decreasing the brightness in the scene affects the quality of the image. This is due to the fact that the combination of lens interfaces that was created produces dimmer images than, for example, a standard perspective camera with a field of view of  $75^\circ$ . This difference can be observed in Figure 7.

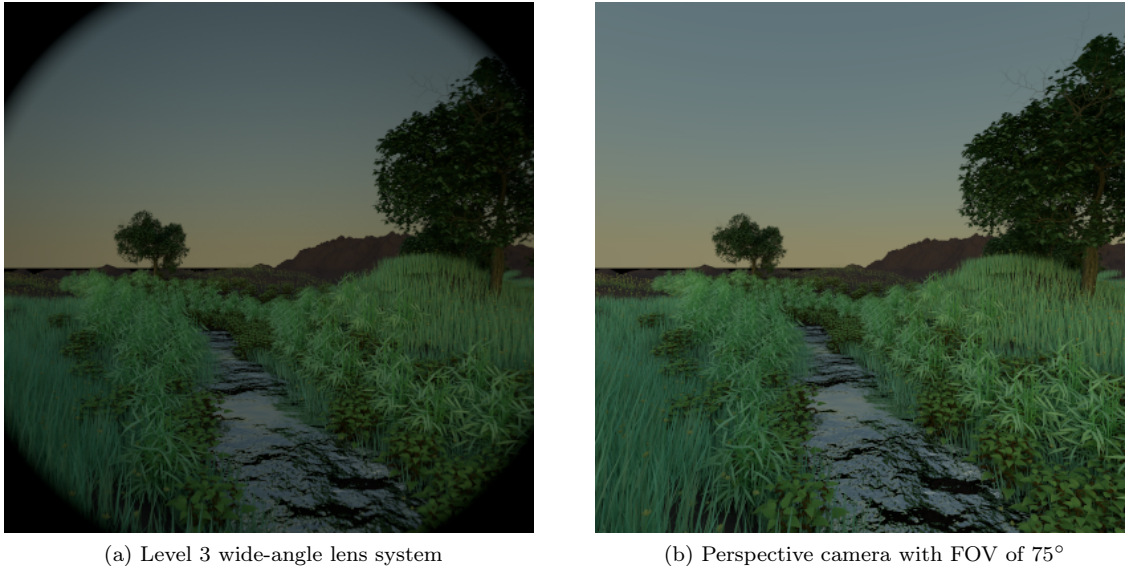


Figure 7: Slight difference in the brightness of the scene between our realistic lens system and the standard perspective camera

In order to show how certain lens system captures different parts of the scene, three distinctive angles of view were used. Renders with  $0^\circ$ ,  $45^\circ$ , and  $90^\circ$  degrees viewing angles, in reference to the center of the scene, were generated. Figure 8 shows renders of different viewing angles for the indoor scene in the high brightness environment. Furthermore, we have to emphasize the distortions that are occurring in the final rendering when wide-angle cameras are used. Thus, moving from the center of the image produces visible distortions. In other words, with distance from the optical axis, imaging magnification decreases and thus resulting in barrel distortion.

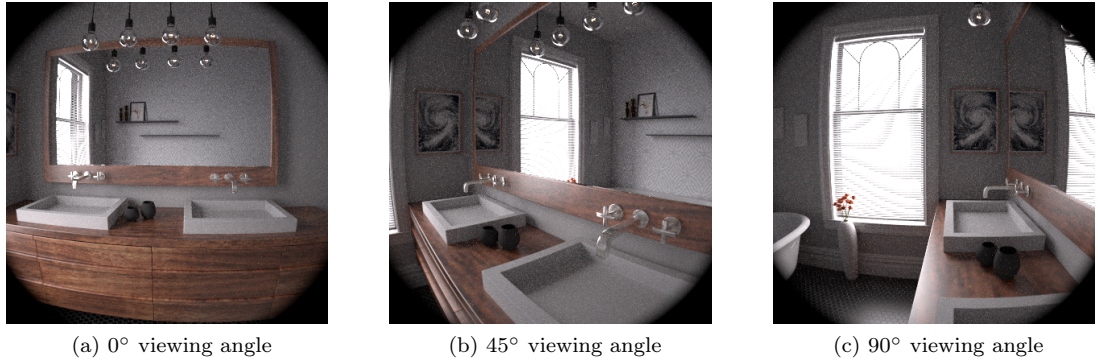


Figure 8: Scene rendered with the same camera but with a different horizontal viewing angle

In Figure 9, five different images that were generated with different FOVs are shown. In order to create a better distinction between different lens system, the indoor scene with high brightness environment and 45° viewing angle was used as a reference. So, we can observe that as we progress from Level 1 to Level 5, more objects become visible in the scene. This is consistent with the theory elaborated in Section 1. Additionally, the main artifact in the rendering images that can be observed is the distortion. This was already discussed, but with using a differently created lens system this becomes more pronounced. In Level 1, the lens system barrel distortion is almost non-existent. On the other hand, Level 5 lens system shows heavier distortion happening as we move from the optical axis.

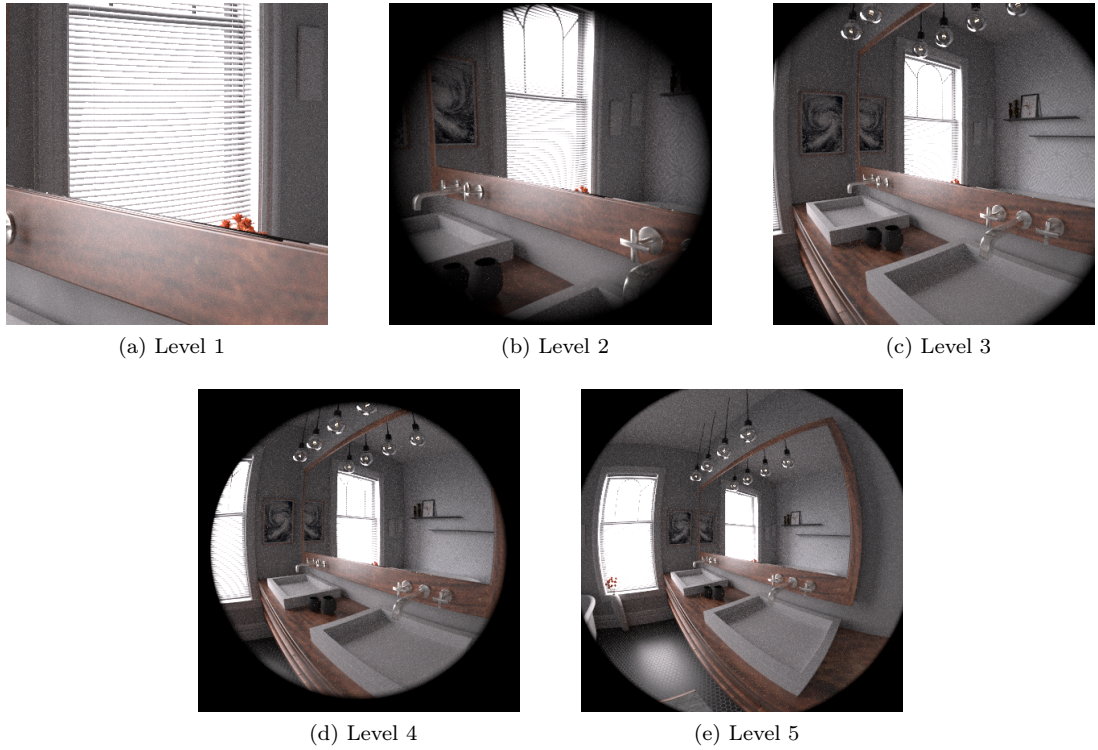


Figure 9: Different wide-angle camera levels used to render the indoor scene

To better appreciate the distortions that may occur when using the created lens system, Figure 10 is generated. Here, using a level 3 camera lens system, image distortions near the edge of the image can be observed. The green lines are located in the center of the image, and for them, only a slight distortion can be seen. On the other hand, as we move closer to the image edge, the red lines are visualized. These lines have more pronounced curvature, and they show bigger distortion. From this figure, it can be deduced that the lines of the scene that are not radially placed with respect to the center of the scene will be affected by the image distortion as their location is nearer to the edge of the FOV.

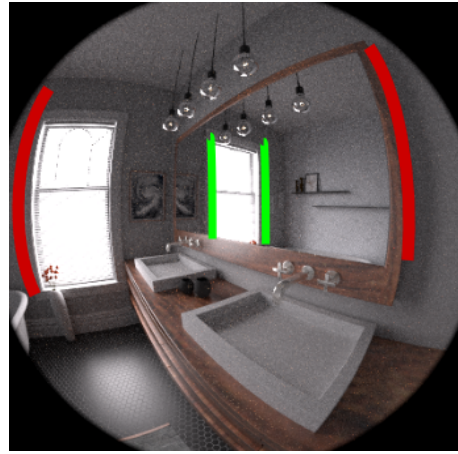


Figure 10: Curvature of straight lines with respect to their position and orientation from the center of the image

Additionally, this is even more noticeable when using different viewing angles. Figure 11 shows occurring distortions for the same line, just in different viewing angles. As we horizontally move around the center of the scene, the position of the line is changing in the rendered image. Therefore, the red line on the first image manifests the biggest distortion and curvature. This line is not radial to the center of the image and is located farther from the center. On the other hand, as the viewing angle increases, the line is moving closer to the center of the image and is more radially placed with regard to the center of the image. This results in decreasing the intensity of the distortion, and the green line is presented as almost perfectly straight.



Figure 11: Curvature of straight lines with respect to the viewing angle

## 4. Conclusions

In this work, a simulation of different wide-angle cameras using PBRT-V3 API has been implemented. We started using as a base one of the realistic lenses available in the Scenes Library, and through the systematic addition and removal of lens interfaces, we have simulated different wide-angle cameras with different FOV and Focal Length properties. So, we have created 5 different wide-angle cameras with a focal length between 50mm and 10mm. Each of these 5 cameras was tested to generate different scenes under different conditions. So, we tested them in both indoor and outdoor scenes. This allowed us to simulate the performance of our cameras in both tight space scenes and wide landscape scenes. Also, in both cases, we vary the lighting and the position/angle of the camera. In order to be able to perceive the change of the scene captured by our different wide-angle lenses.

In the results, we clearly noticed some particular characteristics in each of the cameras used. For example, we noticed how as we increased the FOV the number of objects on the screen also increased. But, in order to display more objects on the screen, these cameras must decrease the perceived size of the displayed objects. Thus, we could also notice that as we increase the FOV, distortions appear progressively that give the sensation of a curved scene. Thus, due to very large FOVs, fisheye cameras can be produced. Finally, as future work, we propose to carry out the experiment of creation and simulations of wide-angle cameras using a more theoretical approach. Since in our experiment we focused on generating our cameras using an empirical approach instead of delving into the mathematical and physical formulas related to lens systems.

## 5. Contributions

The workload of this project was divided in the following way between team members:

- Dong Han

He was in charge of the investigation of the theoretical foundations of the realistic cameras and the writing of the introduction. He also collaborated in the rendering of different scenes.

- Ronny Velastegui

He was in charge of project coordination. He prepared the general methodology, as well as investigating and developing the 5 realistic wide-angle camera levels in PBRT.

- Milan Kresović

He was in charge of the rendering and modification of the scenes in which the different cameras were tested, as well as the analysis of the results.

## References

- [1] J. D. Foley, A. Van Dam, S. K. Feiner, J. F. Hughes and R. L. Phillips, *Introduction to computer graphics*. Addison-Wesley Reading, 1994, vol. 55.
- [2] C. Kolb, D. Mitchell and P. Hanrahan, ‘A realistic camera model for computer graphics,’ in *Proceedings of the 22nd annual conference on Computer graphics and interactive techniques*, 1995, pp. 317–324.
- [3] <https://av.jpn.support.panasonic.com/support/global/cs/dsc/knowhow/knowhow12.html>.
- [4] T. Kouyama, A. Yamazaki, M. Yamada and T. Imamura, ‘A method to estimate optical distortion using planetary images,’ *Planetary and Space Science*, vol. 86, pp. 86–90, 2013.
- [5] Pharr, ‘Introduction,’ in *Physically Based Rendering: From Theory to Implementation, Third Edition*, Morgan Kaufmann/Elsevier, 2017.
- [6] <http://kadie.me/lenses/>.
- [7] *Scenes for pbrt-v3*. [Online]. Available: <http://www.studios-cad.fr/galerie.html> (visited on 29/09/2020).
- [8] *La galerie des réalisations, studio s.* [Online]. Available: <http://www.studios-cad.fr/galerie.html> (visited on 28/11/2020).
- [9] O. Deussen, P. Hanrahan, B. Lintermann, R. Měch, M. Pharr and P. Prusinkiewicz, ‘Realistic modeling and rendering of plant ecosystems,’ in *Proceedings of the 25th annual conference on Computer graphics and interactive techniques - SIGGRAPH '98*, ACM Press, 1998. DOI: [10.1145/280814.280898](https://doi.org/10.1145/280814.280898). [Online]. Available: <https://doi.org/10.1145/280814.280898>.